Diffusion of Green Fluorescent Protein in the Aqueous-Phase Lumen of Endoplasmic Reticulum

Mark J. Dayel,* Erik F. Y. Hom,# and A. S. Verkman*

*Departments of Medicine and Physiology, Cardiovascular Research Institute, and #The Graduate Group in Biophysics, University of California, San Francisco, California 94143-0521 USA

ABSTRACT The endoplasmic reticulum (ER) is the major compartment for the processing and quality control of newly synthesized proteins. Green fluorescent protein (GFP) was used as a noninvasive probe to determine the viscous properties of the aqueous lumen of the ER. GFP was targeted to the ER lumen of CHO cells by transient transfection with cDNA encoding GFP (S65T/F64L mutant) with a C-terminus KDEL retention sequence and upstream prolactin secretory sequence. Repeated laser illumination of a fixed 2-μm diameter spot resulted in complete bleaching of ER-associated GFP throughout the cell, indicating a continuous ER lumen. A residual amount (<1%) of GFP-KDEL was perinuclear and noncontiguous with the ER, presumably within a pre- or cis-Golgi compartment involved in KDEL-substrate retention. Quantitative spot photobleaching with a single brief bleach pulse indicated that GFP was fully mobile with a $t_{1/2}$ for fluorescence recovery of 88 ± 5 ms (SE; 60× lens) and 143 ± 8 ms (40×). Fluorescence recovery was abolished by paraformaldehyde except for a small component of reversible photobleaching with $t_{1/2}$ of 3 ms. For comparison, the $t_{1/2}$ for photobleaching of GFP in cytoplasm was 14 ± 2 ms (60×) and 24 ± 1 ms (40×). Utilizing a mathematical model that accounted for ER reticular geometry, a GFP diffusion coefficient of 0.5–1 × 10^{-7} cm^2/s was computed, 9–18-fold less than that in water and 3–6-fold less than that in cytoplasm. By frequency-domain microfluorimetry, the GFP rotational correlation time was measured to be 39 ± 8 ns, ~2-fold greater than that in water but comparable to that in the cytoplasm. Fluorescence recovery after photobleaching using a 40× lens was measured (at 23°C unless otherwise indicated) for several potential effectors of ER structure and/or lumen environment: $t_{1/2}$ values (in ms) were 143 ± 8 (control), 100 ± 13 (37°C), 53 ± 13 (brefeldin A), and 139 ± 6 (dithiothreitol). These results indicate moderately slowed GFP diffusion in a continuous ER lumen.

INTRODUCTION

The diffusion of solutes in intracellular aqueous compartments is essential for a number of cellular processes including enzyme-substrate reactions in the cytoplasm and mitochondria, and replication and nucleic acid transport in the nucleus. In the endoplasmic reticulum (ER), diffusion could be an important factor influencing protein folding and membrane protein translocation events (Simon et al., 1992). The ER lumen is densely filled with small solutes (e.g., calcium and glutathione) and proteins (e.g., lipid synthases and molecular chaperones) at very high concentrations (100–200 mg protein/ml) (Koch et al., 1987; Helenius et al., 1992; Hammond and Helenius, 1995). It is not known, however, whether molecular crowding in the ER lumen is an important determinant and potential regulator of protein transport and posttranslational processing.

The rheological properties of cellular aqueous compartments has been a subject of longstanding interest. Initial studies of cytoplasmic viscosity utilized exogenously added magnetic resonance and fluorescent probes. Fluorescence recovery after photobleaching (FRAP) measurements of microinjected fluorescein isothiocyanate-labeled (FITC)-dextrans and FITC-Ficolls of molecular size $<10^6$ Da showed translational mobilities only a fewfold slower in cytoplasm than in water, but substantially slower for much larger molecules (Luby-Phelps et al., 1987; Seksek et al., 1997). Spot photobleaching of the small chemical fluorophore BCECF indicated that compared to its translational diffusion in water, BCECF diffusion was slowed 3–4-fold in bulk cytoplasm (Kao et al., 1993) and membrane-adjacent cytoplasm (Swaminathan et al., 1996). Analysis of individual factors responsible for the slowed BCECF diffusion indicated that the primary barrier to BCECF translation is molecular crowding, with lesser effects of BCECF binding to cellular components and increased local microviscosity (the apparent local viscosity in the absence of binding or collisional interactions) (Kao et al., 1993). Measurements of cytoplasmic microviscosity by BCECF rotation (Fushimi and Verkman, 1991; Bicknese et al., 1993) and by the use of viscosity-sensitive fluorophores (Luby-Phelps et al., 1993) indicated a microviscosity at most 1.5-fold that of water.

The molecular cloning of green fluorescent protein (GFP) has permitted noninvasive measurements of probe mobility with excellent targeting specificity and suitable optical properties for photophysical studies (reviewed in Verkman, 1999). GFP has been targeted to multiple organelles (Rizzuto et al., 1995; Degiorgi et al., 1996; Gerdes and Kaether, 1996; Ellenberg et al., 1997; Presley et al., 1997; Kneen et al., 1998) and used to follow the slow diffusion of membrane proteins in plasma membranes and organelles (Cole et

Received for publication 26 August 1998 and in final form 2 February 1999.

Address reprint requests to Alan S. Verkman, M.D., Ph.D., 1246 Health Sciences East Tower, Cardiovascular Research Institute, University of California, San Francisco, San Francisco, CA 94143-0521. Tel.: 415-476-8530; Fax: 415-665-3847; E-mail: verkman@itsa.ucsf.edu; http://www.ucsf.edu/verklab.

0006-3495/99/05/2843/09 $2.00

al., 1996; Barak et al., 1997). An initial study evaluated GFP as a probe of translational and rotational dynamics in cytoplasm using photobleaching recovery and time-resolved anisotropy methods (Swaminathan et al., 1997). GFP was found to be a suitable probe of solute translation with the caveat that (diffusion-independent) reversible GFP recovery after photobleaching involving triplet state relaxation is sometimes detected. GFP translational diffusion in the cytoplasm was similar to that of a microinjected FITC-dextran of comparable size. As measured by time-resolved anisotropy, GFP rotation was found to provide an excellent index of local viscosity because of the absence of intramolecular depolarizing rotations of the GFP triamino acid chromophore. Recently, GFP was used as a probe to measure viscosity in the mitochondrial matrix (Partikian et al., 1998). Mathematical models were developed to deduce absolute diffusion coefficients from photobleaching studies of fluorophore diffusion in the aqueous lumen of cellular organelles having complex geometries (Ölveczky and Verkman, 1998).

A goal of this study was to determine whether the crowded ER lumen restricts the translational and rotational diffusion of a protein-size molecule. GFP was used as a probe of solute mobility in the ER lumen because of its excellent targeting specificity to the ER lumen, minimal binding interactions with cellular components, and suitable optical properties for quantitative photobleaching and time-resolved anisotropy measurements. It was found that GFP is freely diffusible throughout the ER lumen, but that its diffusion is 9–18-fold slower than in water and 3–6-fold slower that in the cytoplasm, with minimal binding to ER luminal contents. The quantitative methods developed here were subsequently used to evaluate the consequences of several conditions and effectors that have been proposed to modify ER structure and/or luminal environment.

METHODS

Cell culture and transfection

CHO-K1 cells (ATCC CRL9618) were grown on 18-mm diameter round glass coverslips in a 95% air, 5% CO_2 incubator at 37°C in Ham's F12 medium containing 10% fetal bovine serum, 100 units/ml penicillin, and 100 mg/ml streptomycin. Cells were transfected 1 day after plating just before confluence was reached. Cells in each well of a six-well plastic dish containing a coverglass were transfected with a mixture consisting of 1 μg plasmid DNA encoding an ER-targeted GFP-fusion construct within the vector pcDNA3.1(+) (Invitrogen Corp., Carlsbad, CA) and 12 μg lipofectamine (Life Technologies, Gaithersburg, MD) in a 0.2-ml volume of OPTI-MEM (Life Technologies). After 5 h the transfection mixture was replaced with 1 ml culture medium. Cell were used 2 days after transient transfection. As reported previously (Kneen et al., 1998), the ER-targeting construct consisted of the EGFP coding sequence (Clontech Laboratories, Inc., Palo Alto, CA) cloned downstream from the preprolactin signal sequence, in which a KDEL ER-retention/retrieval sequence was inserted just before the stop codon in the GFP cDNA. Immunofluorescence showed colocalization of GFP fluorescence with staining by an antibody against the ER resident protein GRP94 (Tamarappoo and Verkman, 1998).

Fluorescence recovery after photobleaching

FRAP measurements were carried out on an apparatus described previously (Kao and Verkman, 1996) with slight modifications. An argon ion laser beam (488 nm; Innova 70–4, Coherent Inc., Santa Clara, CA) was modulated by an acousto-optic modulator (Brimrose, Inc., Baltimore, MD; 1.5 μs response time) and directed through an objective onto the stage of an inverted epifluorescence microscope (Diaphot, Nikon Inc., Melville, NY). An electronic shutter was introduced in the excitation pathway to completely eliminate sample illumination as needed. The microscope was also equipped for full-field epiillumination to visualize all cells to target the focused laser beam. The full-field and laser beams were reflected by a dichroic mirror (510 nm) onto the sample by an objective lens (Nikon 100× oil Fluor, N.A. 1.4; 60× oil Fluor, N.A. 1.4; 40× oil Fluor, N.A. 1.3). For measurements performed at 37°C the objective was heated by a commercial thermoregulator (Bioptechs Inc., Butler, PA) and the sample chamber was heated by a home-built heating coil with thermocouple temperature feedback. For most experiments, the laser beam power was set to 200–500 mW (488 nm) and the attenuation ratio (the ratio of bleach to probe beam intensity) was set to 5000–15000. Sample fluorescence was filtered by serial barrier (Schott glass OG 515) and interference (530 $\pm$ 15 nm) filters and detected using a photomultiplier and 14-bit analog-to-digital converter. A gating circuit transiently decreased photomultiplier gain during photobleaching. Fluorescence was sampled every 0.2 s for 4 s before the bleach pulse; subsequently, sampling was performed over three different time intervals specified as follows: high-resolution data (1 MHz sampling rate) generally over 500 ms, low-resolution data (generally 10^4 points) over 0.5–5 s, and late-time data (0.2 s sampling time every 1–4 s). For FRAP measurements in the ER, 15–25 individual fluorescence recovery curves (each from a different cell) were averaged, and the data set was repeated 4–10 times using different transfections.

Cell preparations

Transfected cells grown on glass coverslips were placed in a home-built perfusion chamber and flushed with Ham's F12 phenol red-free medium. Photobleaching measurements were generally performed within 30–60 min. In some experiments, cells were preincubated with brefeldin A (5 mM, 5 h, 37°C), dithiothreitol (1 mM, 3 h, 37°C), or the calcium ionophore A23187 (5 mM, 10 min, 23°C). In other experiments, cells were incubated for 10 min at 23°C with hyperosmolar media (containing added sucrose) or hypoosmolar media (contained added water).

Analysis of FRAP data

As described in the Appendix and a previous paper (Ölveczky and Verkman, 1998), fluorophore diffusion coefficients (D, in cm^2/s) were determined from recovery half-times ($t_{1/2}$) (time at which fluorescence recovers by 50%) using a mathematical model of diffusion in an ER composed of plates or interconnected cylinders. The $t_{1/2}$ values were determined by nonlinear least-squares fit of recovery data $F(t)$ to a semiempirical equation reported previously (Feder et al., 1996): $F(t) = F_0 + [F_0 + R(F_{init} - F_0)](t/t_{1/2})^\alpha/[1 + (t/t_{1/2})^\alpha]$, where R is the fractional fluorescence recovery and α is an empirical exponent related to anomalous diffusion (Periasamy and Verkman, 1998). The $t_{1/2}$ values for the recovery data in this paper were found to be insensitive to the fitting method, with similar values (generally <5% difference) obtained by a different method described by Swaminathan et al. (1997).

Time-resolved anisotropy measurements

Fluorescence lifetime and anisotropy decay measurements were performed using a Fourier Transform Fluorimeter (48000 MHF, SLM Instruments Inc., Urbana, IL) in which epifluorescence microscopy optics replaced the cuvette compartment (Fushimi and Verkman, 1991). The impulse-modulated, vertically polarized light (488 nm) was reflected onto the sample by

a 510-nm dichroic mirror and objective lens; emitted fluorescence was filtered by a 515-nm cut-on filter and passed through a rotatable analyzing calcite polarizer. Analysis of lifetime and time-resolved anisotropy were conducted by a comparative approach as described previously (Verkman et al., 1991). Fluorescein in 0.1 N NaOH was used as a 4.0-ns lifetime standard. Anisotropy decay measured by microscopy required the inclusion of a geometric factor (generally ~1.3) to correct for the differential detection of parallel versus perpendicular emission polarization arising mainly from differential reflectivity of the dichroic mirror.

Photobleaching with widefield or confocal image detection

A Nipkow wheel confocal microscope (Leitz upright microscope with Technical Instruments K2-Bio coaxial-confocal attachment) and cooled CCD camera detector (Photometrics Inc., Tucson, AZ) were used to acquire cell images after bleaching. An electronically shuttered bleach beam from the argon laser was directed onto the cell sample from below using a Leitz 25× long-working-distance air objective. The beam diameter in the sample plane was controlled by adjusting the objective z-position. Cells were viewed from above by epifluorescence using a 100× oil immersion objective and GFP filter set. Software was written to coordinate the bleach pulse, excitation and camera shutters, and image acquisition.

RESULTS

Photobleaching imaging experiments were carried out on transfected CHO cells expressing GFP in the ER lumen. Fig. 1 *A* contains a series of micrographs showing the cellular distribution of GFP before and at different times after photobleaching. The distribution of GFP is clearly reticular and indicative of ER localization. A large bleach spot (*upper left panel*) was used to bleach a substantial fraction of cellular GFP. The darkened zone produced by the bleach pulse was progressively filled in with unbleached GFP diffusing into the bleach zone by diffusion through the ER lumen. By 50 s, GFP fluorescence appears uniformly distributed throughout the cell ER. As expected for irreversible bleaching of GFP, the final whole cell fluorescence of the bleached cell is clearly less than that of an adjacent unbleached cell (*arrow*). The apparently complete ER redistribution of GFP after photobleaching suggests that most, if not all, of the GFP is mobile.

Fig. 1 *B* shows the results of a similar experiment after cell fixation with paraformaldehyde, an amine-reactive agent that is predicted to immobilize all proteins. GFP was bleached with comparable efficiency after paraformaldehyde fixation; however, recovery of fluorescence in the bleached region was not observed. Thus the fluorescence recovery in Fig. 1 *A* can be attributed to GFP diffusion.

To test directly for ER lumen continuity, a small spot located on a single cell was bleached by repeated pulsed laser illumination. Fig. 2 shows that almost all fluorescence throughout the cell could be eliminated by point bleaching. The fluorescence of an adjacent cell (*arrow*) was not diminished, indicating that the reduction in fluorescence throughout the bleached cell resulted from GFP diffusion through a continuous ER lumen and not from a broad laser beam profile. At high camera gain, a small (<1%) amount of residual fluorescence after bleaching was seen with perinuclear locale and Golgi-like pattern (Fig. 2, *right panel*), consistent with models for the recycling of KDEL-tagged proteins (see Discussion). Nonetheless, in the steady state the vast majority of GFP was localized to the ER lumen.

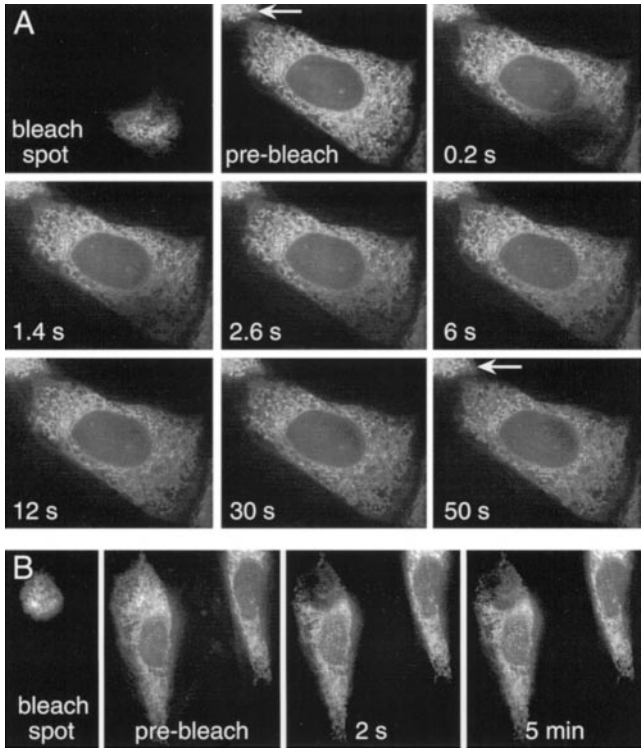

FIGURE 1 Photobleaching of GFP in the ER lumen. (*A*) Serial epifluorescence micrographs of a CHO cell expressing GFP in the ER lumen. The bleach beam profile is shown in the upper leftmost panel. Micrographs are shown before bleaching (pre-bleach) and at indicated times after bleaching (bleach time 200 ms). An adjacent unbleached cell is indicated by an arrow. (*B*) Same as in (*A*) except that cells were fixed by incubation in 4% paraformaldehyde for 60 min before photobleaching.

Spot photobleaching was performed for quantitative analysis of GFP diffusion. Fig. 3 *A* shows representative fluorescence recovery curves for the bleaching of GFP in the ER lumen with the indicated objective lenses producing different spot sizes. The bleach times for these studies were selected to be much less than the observed recovery times (see figure legend). GFP fluorescence recovered to well above 90% of the initial fluorescence, again suggesting that GFP diffuses within a continuous ER lumen. As expected, the fluorescence recovery rates depended strongly on beam spot size with $t_{1/2}$ values of 22 ± 3 ms, 88 ± 5 ms, and 143 ± 8 ms for 100×, 60×, and 40× lenses, respectively. For comparison, Fig. 3 *B* shows similar bleaching studies in cells containing GFP throughout their aqueous-phase cytoplasm and nucleus; $t_{1/2}$ values (in ms) were 6.0 ± 0.5 (100×), 14 ± 2 (60×), and 24 ± 1 (40×). For the 60× and 40× lenses, $t_{1/2}$ values for the ER were ~6-fold greater than for the cytoplasm, suggesting slowed diffusion of GFP in the ER (see below).

Fig. 3 *C* shows fluorescence recovery curves for fixed cells containing GFP in the ER lumen or cytoplasm (note

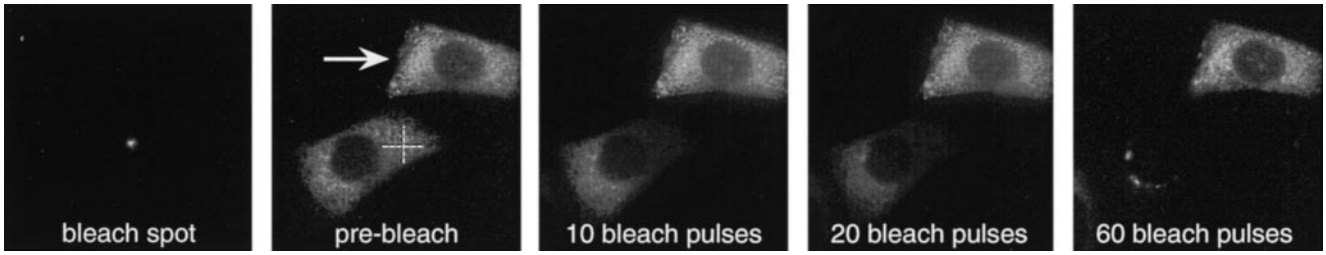

FIGURE 2 Evidence that the ER lumen is continuous. A single spot (at crosshairs) was repeatedly illuminated (200 ms illumination every 2 s) with an intense laser beam. Images were obtained after indicated number of illumination pulses. The arrow indicates an adjacent unbleached cell. Residual perinuclear, Golgi-like fluorescence is seen under high camera gain after 60 bleach pulses (*right panel*) (see text).

different time scale). Although the majority of fluorescence recovery was abolished over long times, there existed a transient ($t_{1/2}$, 3 ± 1 ms) fluorescence recovery whose rate did not depend on laser spot diameter. Further experiments showed that the transient recovery could be produced by relatively low bleach intensities for short bleach times (not shown). As described previously for fluorescein (Periasamy et al., 1996) and GFP (Swaminathan et al., 1997), the rapid fluorescence recovery probably arises from reversible GFP photobleaching due to triplet state relaxation. Because the recovery time for reversible GFP photobleaching is very short and independent of bleach spot size, subsequent experiments were conducted with a 40× objective ($t_{1/2}$ of 100–150 ms for irreversible photobleaching) to be able to neglect the reversible photobleaching process.

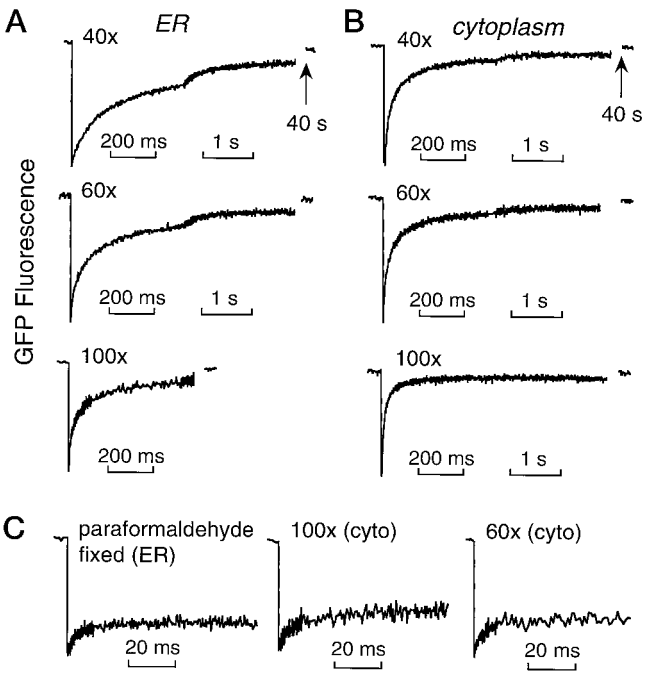

FIGURE 3 Spot photobleaching of GFP in the ER and cytoplasm. (*A*) Bleaching of cells expressing GFP in the ER lumen with indicated objective lenses. Bleach times were 2 ms (40×), 1 ms (60×), 0.3 ms (100×); bleach depth was 25–28%. (*B*) Same as in (*A*) but with cells expressing GFP uniformly in cytoplasm and nucleus (cells described in Swaminathan et al., 1997). (*C*) Same as in (*A*) but after paraformaldehyde fixation. See text for fitted $t_{1/2}$ values.

The diffusion of GFP through the ER lumen of defined geometry was modeled to estimate an absolute GFP translational diffusion coefficient (D) from photobleaching recovery data. Previously, the ER was modeled as a reticulum of orthogonally interconnected cylinders of specified diameter and density (Ölveczky and Verkman, 1998). The principal conclusion of those Monte Carlo computations was that the confinement of fluorophores to a tubular ER geometry had a small effect on their apparent diffusion. At constant D, the apparent recovery $t_{1/2}$ was slowed <1.5-fold for GFP confined to the ER lumen versus GFP uniformly distributed in a slab simulating cell geometry. To validate the robustness of this conclusion based on interconnected cylinders, additional computations were performed for a ribbonlike geometry in which GFP is confined within narrow planes.

The ribbonlike geometry was modeled as described in the Appendix. Fig. 4 *A* shows the geometry in which a bleach beam of diameter d intersects a thin slab containing GFP oriented at an angle θ with respect to the horizontal. The fluorescence recovery time course $F(\tau)$ ($\tau = Dt/d^2$ is a reduced dimensionless time) was computed by numerical integration of the point source solution to the diffusion equation over an ellipse (minor axis $d/2$, major axis $d/2 \cos \theta$) at each time point. Fig. 4 *B* gives $F(\tau)$ for different angles θ. As θ increases, the recovery slows due to the greater mean path a diffusing particle must travel to reach the center of the bleach spot. However, the effect is relatively small because the minor axis of the ellipse is independent of slab orientation. Fig. 4 *C* shows a minor influence of a random distribution of slab orientations. Fig. 4 *D* summarizes correction factors, $1 + (\Delta t_{1/2}/t_{1/2})$, which account for the confinement of GFP to the ER lumen. For example, a correction factor of 1.2 indicates that the apparent $t_{1/2}$ recovery time is increased 1.2-fold for GFP confined in the ER lumen versus uniformly distributed GFP. The range of correction factors for ribbonlike geometry, 1–1.4, is similar to that of 1–1.5 reported for the interconnected cylinder geometry. A more conservative range of the correction factors would be 1–2, presuming that recovery data were obtained from samples with ER sheets that were nonrandomly oriented with respect

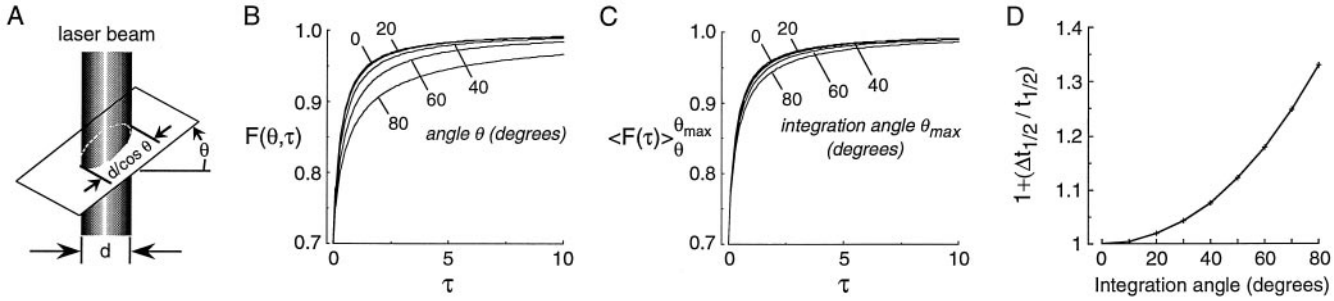

FIGURE 4 Quantitative determination of diffusion coefficients from photobleaching data. (*A*) Sheetlike ER geometry showing laser beam of diameter d intersecting a slab containing GFP oriented at angle θ with respect to the horizontal. (*B*) $F(\theta, \tau)$ computed from Eq. A4 at indicated angles θ. (*C*) $\langle F(\tau) \rangle$ computed from Eq. A5 for randomly oriented slabs from 0° to angle θ_{max}. (*D*) Correction factors $1 + (\Delta t_{1/2}/t_{1/2})$, where $\Delta t_{1/2} = |t_{1/2}(\theta = 0) - t_{1/2}(\theta)|$, for $\theta_{max} = 0-80°$. See Appendix for details.

to the beam axis (see Fig. 4 *B*). Because of uncertainties in the orientation of the ER, a range of D values will be reported corresponding to correction factors of 1–2.

Table 1 summarizes D values for GFP in different aqueous cellular compartments. The deduced D for GFP translational diffusion in the ER was $0.5–1 \times 10^{-7}$ cm^2/s. This value of D is 3–6-fold less than that in cytoplasm, and 9–18-fold less than that for GFP diffusion in water.

The average rotational diffusion of GFP in the ER lumen was measured by time-resolved anisotropy. Fig. 5 shows a representative differential phase-modulation plot for GFP rotation in the ER lumen. The major rotational correlation time was 39 ± 5 ns (SE, four sets of measurements), ~2-fold greater than that of water (20 ns). The absence of a very slow component of GFP rotation suggests that GFP does not bind significantly to the ER wall or to slowly rotating proteins in the ER lumen. A similar measurement of GFP rotation in the ER lumen in paraformaldehyde-fixed cells gave a major rotational correlation time of >100 ns, indicating substantial GFP immobilization. Rotational mobilities of GFP in other cellular aqueous compartments are summarized in Table 1.

The translational diffusion of GFP in the ER lumen was measured in response to various maneuvers that might affect ER geometry and/or matrix environment. Representative fluorescence recovery curves are shown in Fig. 6 *A* and averaged data are summarized in Fig. 6 *C*. In an attempt to change solute concentration in the ER lumen, cells were incubated in anisomolar solutions. There was no significant effect of 150–450 mOsm extracellular solutions (Fig. 6 *C*), a 1.3-fold slowing of GFP diffusion by a 600 mOsm solution, and a more marked effect of a 900 mOsm solution. The lack of a significant change of GFP diffusion in the ER in the presence of 150–450 mOsm extracellular solutions is in contrast with the 4–6-fold change observed for cytoplasmic GFP diffusion (Swaminathan et al., 1997).

Photobleaching measurements performed at 37°C ($t_{1/2}$, 100 ± 13 ms) gave a 1.4-fold faster recovery rate compared to 23°C, as expected by the difference in solute diffusion at these temperatures (see Discussion). Incubation of cells with the calcium ionophore A23187, which produced ER vesiculation within 10 s (Fig. 6 *B, middle panel*), resulted in incomplete GFP fluorescence recovery because of the loss of ER continuity. DTT, a disulfide reducing agent that elicits the "unfolded protein response"-associated expansion of the ER compartment in CHO cells (Helenius et al., 1992), did not have a significant effect on GFP diffusion ($t_{1/2}$, 139 ± 6 ms). Brefeldin A, which blocks ER-to-Golgi anterograde vesicle traffic (Klausner et al., 1992; Sciaky et al., 1997), gave a significant 2.5-fold increased rate of GFP fluorescence recovery ($t_{1/2}$, 53 ± 13 ms). However, brefeldin A did not affect ER structure at the light microscopic level (Fig. 6 *B, right panel*).

TABLE 1 Diffusion of GFP in aqueous cellular compartments

	Translational Diffusion		Rotational Diffusion	
	D(cm^2/s)	D(water)/D	τ_c (ns)	τ_c/τ_c(water)
Water	8.7×10^{-7}	1	20 ± 1	1
Cytoplasm	$2.5–3 \times 10^{-7}$	2.9–3.5	36 ± 2	1.8
Mitochondria	$2–3 \times 10^{-7}$	3–4	23 ± 1	1.2
ER	$0.5–1 \times 10^{-7}$	9–18	39 ± 5	1.9

Data taken from Swaminathan et al. (1997), Partikian et al. (1998), and this study.

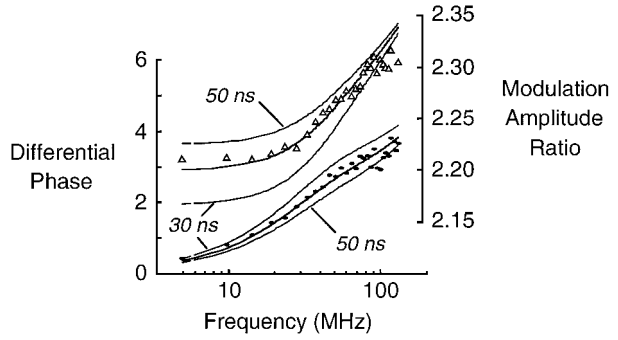

FIGURE 5 Rotational diffusion of GFP in the ER lumen. Differential phase angles (*filled circles*) and modulation amplitude ratios (*open triangles*) for GFP rotation. Fitted rotational correlation times (SE, $n = 4$) were 39 ± 5 ns (fractional amplitude 0.8) and 0.34 ± 0.04 ns. Curves corresponding to correlation times of 30 ns and 50 ns are shown for comparison.

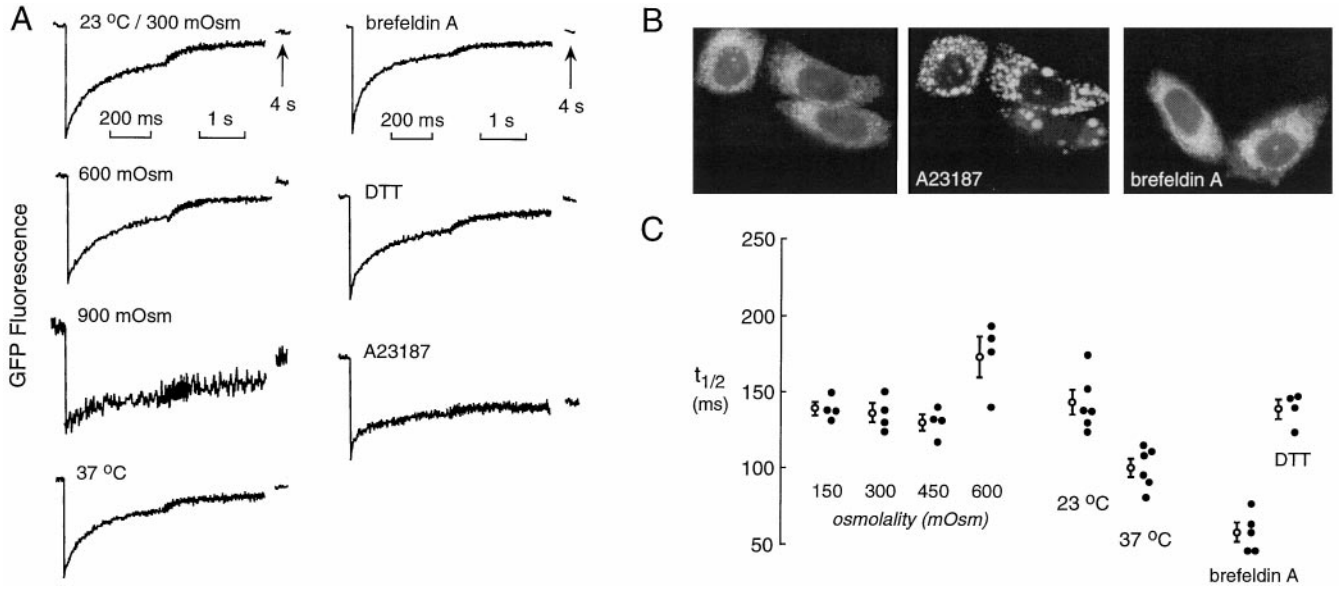

FIGURE 6 Effectors of ER environment of structure. (*A*) Spot photobleaching recovery for cells expressing GFP in the ER lumen for indicated conditions (see Methods for details). Bleach time was 2 ms and bleach depth was 25–28%. (*B*) Fluorescence micrographs before (*left*) and after 10 s incubation with A23187 (*middle*), and after incubation with brefeldin A (*right*). (*C*) Summary of recovery $t_{1/2}$ values. Each point is the average of data from 15–25 individual cells.

DISCUSSION

A principal finding of this study was that GFP, an ~30-kDa protein, diffuses freely throughout the ER lumen, but that its diffusion is slowed moderately ($D = 0.5–1 \times 10^{-7}$ cm^2/s). GFP rotational diffusion in the ER lumen was 2-fold slower than in water, whereas GFP translational diffusion was 9–18-fold slower in the ER versus water and 3–6-fold slower versus the cytoplasm. The rate of GFP translational diffusion formally represents a lower limit to ER diffusion because it assumes no GFP binding and incorporates a minor correction for ER geometry. The time-resolved anisotropy measurements supported the validity of the assumption about little GFP binding, and the mathematical modeling addressed the issue about ER geometry (see below). As discussed with respect to GFP diffusion in cytoplasm and mitochondria (Swaminathan et al., 1997; Partikian et al., 1998), the greater slowing of GFP translation versus rotation is probably related to collisional interactions that occur during translation.

In a study by Terasaki et al. (1996), photobleaching measurements of GFP diffusion were done to assess the effects of cellular calcium and fertilization on ER structure and continuity in starfish eggs. However, they did not quantify the diffusion coefficient of GFP for the purpose of relating it to the physicochemical environment in the ER lumen. In a photobleaching study by Subramanian and Meyer (1997), the diffusion coefficient of a 60-kDa ER-targeted elastase-GFP fusion protein was measured to be ~0.05×10^{-7} cm^2/s. However, the influence of binding interactions on the elastase-GFP diffusion coefficient was not considered. Their estimated elastase-GFP diffusion coefficient is 10–20 times smaller than that reported here for GFP alone (half the molecular weight of elastase-GFP). Assuming spherically distributed mass and free diffusion, one would expect a 1.26-fold slower diffusion of elastase-GFP versus GFP. Assuming a more realistic model of the proteins as prolate ellipsoids and that elastase-GFP is 2–3 times more prolate than GFP, Perrin's equations (Cantor and Schimmel, 1980) would predict an even smaller difference in the diffusion of elastase-GFP versus GFP. It is thus likely that elastase-GFP is extensively bound and/or significantly geometrically constrained in the ER lumen. We think it unlikely that the very different diffusion coefficients arise from cell type differences: Subramanian and Meyer conducted their studies using rat leukemia 2H3 and mouse fibroblast 3T3 cells, whereas the experiments here were done on Chinese Hamster Ovary cells. Nonetheless, we emphasize the importance of performing time-resolved fluorescence anisotropy measurements in conjunction with photobleaching experiments to clarify such issues.

A small component of reversible GFP photobleaching was detected in the spot photobleaching measurements. It was seen as a very fast fluorescence recovery ($t_{1/2}$ of ~3 ms), which was independent of bleach spot size and thus unrelated to GFP diffusion. Similar reversible GFP photobleaching was observed for photobleaching of expressed GFP in cytoplasm and purified GFP in viscous saline solutions (Swaminathan et al., 1997). Reversible recovery is thought to arise from population of the triplet state during the bleach pulse, followed by relaxation to the S_0 ground state during the recovery period producing increasing fluorescence. For fluorescein, the recovery due to triplet state relaxation can be made immeasurably fast by addition of triplet state quenchers such as O_2 and Mn^{2+} (Periasamy et

al., 1996); however, such maneuvers do not affect GFP photobleaching because of the inaccessibility of the buried triamino acid chromophore to small molecules (Yang et al., 1996; Ormø et al., 1996; Swaminathan et al., 1997). The reversible photobleaching was not seen in the imaging experiments of fixed cells because the images were acquired well after the reversible component was complete. For measurements conducted with a 40× objective, the time course of recovery from irreversible GFP photobleaching was well resolved (>25-fold slower) from that of the recovery from reversible photobleaching.

The determination of absolute diffusion coefficients from photobleaching recovery data required modeling of ER geometry and made the assumption of a single time-independent diffusion coefficient. The confinement of GFP to the ER lumen is predicted to result in mildly slowed fluorescence recovery compared to the situation in cytoplasm or aqueous solution layers in which GFP is distributed homogeneously over three dimensions. Computation of a "correction factor" for ER geometry requires knowledge of the ER geometry. Precise three-dimensional reconstructions of ER geometry are needed using electron microscopy tomography or other approaches. Current descriptions of ER geometry derived from conventional transmission electron microscopy depict the ER lumen as layers of planar ribbons or interconnected cylinders that vary with cell type and position within the cell (Alberts et al., 1994). The modeling described here and by Ölveczky and Verkman (1998) indicated that small (<1.5-fold) correction factors are needed even when very different assumptions are made about ER geometry. The robustness of the modeling suggests that the computed absolute D value ranges are reasonably accurate. The issue of heterogeneity in diffusion coefficients and anomalous diffusion in the ER lumen is difficult to address using the available data. We recently developed analysis procedures to deduce complex diffusive phenomena from photobleaching recovery data (Periasamy and Verkman, 1998); however, the complexity of ER geometry and the relatively poor signal-to-noise ratio in individual fluorescence recovery curves precluded the use of these procedures.

Repeated bleaching of a single spot (Fig. 2) demonstrated that the ER lumen was continuous and that almost all of the observed GFP fluorescence was associated with the ER reticular network. The <1% residual fluorescence most likely arises from a pre-Golgi or cis-Golgi compartment based on its pattern of perinuclear localization. This result supports and corroborates biochemical- and electron micrographic-based models of KDEL recycling in which proteins with a C-terminal KDEL amino acid sequence that escape from the ER are returned via an intermediate ER-Golgi compartment (Klausner et al., 1992; Griffiths et al., 1994; Stinchcombe et al., 1995; Sciaky et al., 1997).

Several potential effectors of ER geometry or lumen environment were studied. External solution osmolality was changed in an attempt to alter ER lumen volume, and thus luminal solute concentrations. This maneuver was previously shown to change cell volume effectively (Farinas et al., 1995). Similar experiments for GFP diffusion in the cytoplasm gave 2.9-fold slowing of GFP diffusion for 2-fold cell shrinking and 1.6-fold increased diffusion for 2-fold cell swelling (Swaminathan et al., 1997). The data here showed surprisingly little effect of solution osmolality on GFP diffusion in the ER. We believe that the most likely explanation is that geometric restrictions and/or volume homeostatic mechanisms maintain the constancy of ER luminal volume under the strains of external solution osmolality. Such volume homeostasis might be achieved through cytoskeletal reinforcements such as microtubules, which associate with the ER and are involved in ER reorganization (Terasaki et al., 1986; Lee and Chen, 1988). Experiments using isolated ER membrane vesicles containing expressed GFP will be needed to examine the effect of lumen solute concentration on GFP diffusion.

Increasing temperature from 23 to 37°C produced a small 1.4-fold increase in the rate of GFP diffusion in the ER lumen. The water solvent viscosities at 23°C (0.933 cp) and 37°C (0.692) (Weast, 1986) predict a 1.35 increase in solute diffusion over this temperature range. While it is possible that ER reticular structure is altered by an increase in temperature, it does not seem necessary to invoke this as an explanation for increased GFP diffusion based on the anticipated differences in viscosity.

Increasing cytosolic calcium concentration by the ionophore A23187 produced vesiculation of CHO cell ER and an expected decrease in the fraction of fluorescence recovery in photobleaching measurements. These results are in agreement with those determined using starfish eggs (Terasaki et al., 1996), rat basophilic leukemia 2H3 cells, and mouse fibroblast 3T3 cells (Subramanian and Meyer, 1997).

The reducing agent DTT disrupts disulfide bonding and leads to the unfolding of disulfide-containing proteins in the normally oxidative ER. Most cells treated with DTT mount a so-called unfolded protein response (UPR) characterized morphologically by a gross expansion of the ER compartment. Helenius et al. (1992) have shown by electron microscopy that DTT-treated CHO cells contain proliferated ER compartments. We found that DTT incubation did not significantly affect GFP diffusion in the ER. This suggests that DTT-induced ER expansion occurs in a manner in which the ER luminal density of solutes does not change. In an effort to counter the unfolding effects of DTT, cells up-regulate the synthesis of ER luminal molecular chaperones involved in protein quality control (McMillan et al., 1994). As the ER compartment proliferates, it would be expected that lipid membrane production is concomitantly up-regulated. Indeed, Cox et al. (1997) have demonstrated that the biosynthetic pathways for protein and lipid production in the ER are intimately coupled in yeast during UPR. Our biophysical characterization of solute diffusion in the ER lumen of DTT-treated CHO cells is consistent with these qualitative findings in yeast.

Whereas DTT-treatment resulted in little change in the apparent rate of GFP diffusion in the ER lumen, brefeldin A produced a 2.7-fold increase. The deduced GFP diffusion

coefficient after brefeldin A treatment was $1.4–2.8 \times 10^{-7}$ cm^2/s, slightly less than that for GFP diffusion in cytoplasm. Brefeldin A blocks vesicular traffic from the ER to the Golgi without any gross change in ER ultrastructure at the light microscopic level. We believe the most likely explanation for the increased GFP diffusion in brefeldin A-treated cells is that the inhibition of anterograde vesicle movement without effect on retrograde transport leads to an expansion of the ER compartment in a manner that decreases molecular crowding. In a study on the effects of brefeldin A on Golgi tubule traffic, Sciaky et al. (1997) demonstrated that brefeldin A treatment in CHO cells leads to the collapse of the Golgi compartment onto the ER within ~10 min. We propose that molecular crowding in the ER lumen is decreased by Golgi coalescence with the ER compartment; an increase in the ratio of total ER membrane lipid to total luminal protein results in the dilution of ER luminal contents.

Slowed diffusion of GFP can be viewed as arising from three factors: collisions with obstacles, increased intrinsic viscosity of the medium, and binding interactions (Kao et al., 1993). The greater slowing of translational diffusion as compared to rotational diffusion suggests that the major factor influencing the mobility of GFP in the ER lumen is collisional in nature. The decrease in both translational and rotational mobilities may indicate some component(s) of binding. While a more detailed study would be necessary to delineate the precise contributions of these three factors, the results here establish quantitative methods for determining the mobility of proteins in the ER and provide the groundwork for further studies of ER-related processes.

APPENDIX

Model of solute diffusion in the ER lumen

The ER was modeled as planar sheets, each sheet inclined at an angle θ to the horizontal (see Fig. 4 *A*). The vertically oriented bleach/probe beam was modeled as a uniform disk profile of diameter d. It was assumed that the planar sheets to which GFP is confined are very thin and that bleach time is very brief. The intersection of the bleach/probe beam with each planar sheet produces an ellipse of minor axis $d/2$ and major axis $(d/2)\cos\theta$.

The diffusion equation for *bleached* fluorophore moving *out of* an ellipse (formally identical to unbleached fluorophore moving into an ellipse) was solved numerically by superposition of point source diffusion profiles. The solution of the two-dimensional diffusion equation for a point source is given by Crank (1975)

$$C(\vec{r}, Dt) = (M/4\pi Dt)e^{(r^2/4Dt)} \tag{A1}$$

where M is the amount of bleached fluorophore and D is the diffusion coefficient. Equation A1 can be rewritten in terms of $\tau = Dt/d^2$, a dimensionless time variable:

$$C(\vec{r}, \tau) = (M'/4\pi\tau)e^{(r^2d^2/4\tau)} \tag{A2}$$

where $M' = (M/d^2)$ is the normalized concentration of bleached fluorophore at position $\vec{r}$. The concentration of bleached fluorophore contributed by point sources at a set of positions $\{\vec{r}_p\}$, distributed throughout an ellipse of area E, and observed at a position $\vec{r}_q$ within the ellipse, is given by

$$C(\vec{r}_q, \tau) = \sum_{p\in E} C(|\vec{r}_q - \vec{r}_p|, \tau) \tag{A3}$$

The total fluorescence intensity arising from the elliptical cross-section between a planar sheet of fluorophore at an angle θ and an illuminating beam is then given as the sum over all observation points within the ellipse,

$$F(\theta, \tau) = A \cdot \sum_{q\in E} C(\vec{r}_q, \tau) \tag{A4}$$

where A is a constant relating to bleached fluorophore concentration to fluorescence intensity. For planes of random orientations between angles θ and θ_{max} the total mean fluorescence intensity is given by

$$\langle F(\tau)\rangle_\theta^{\theta_{max}} = \sum_\theta^{\theta_{max}} F(\theta, \tau) \cdot \cos\theta \Big/ \sum_\theta^{\theta_{max}} \cos\theta \tag{A5}$$

Computations were performed in Cartesian coordinates with $\Delta x = \Delta y = d/40$ and $\theta = 2°$. For the case of a horizontal plane yielding a circular cross-sectional area, computed and analytical solutions were indistinguishable using this discretization scheme.

We thank Katherine Chen for cell culture and plasmid preparations, and Drs. Javier Farinas and N. Periasamy for helpful advice.

This work was supported by National Institutes of Health Grants DK43840, HL60288, DK16095, DK35124, and HL59198 and a grant from the National Cystic Fibrosis Foundation.

REFERENCES

Alberts, B., D. Dennis, J. Lewis, M. Raff, K. Roberts, and J. D. Watson. 1994. Molecular Biology of the Cell, 3rd ed. Garland Press, New York. 577–598.

Barak, L. S., S. S. Ferguson, J. Zhang, C. Matenson, T. Meyer, and M. G. Caron. 1997. Internal trafficking and surface mobility of a functionally intact β2-adrenergic receptor-green fluorescent protein conjugate. *Mol. Pharmacol.* 51:177–184.

Bicknese, S., N. Periasamy, S. B. Shohet, and A. S. Verkman. 1993. Cytoplasmic viscosity near the cell plasma membrane: measurement by evanescent field frequency-domain microfluorimetry. *Biophys. J.* 165: 1272–1282.

Cantor, C. R., and P. R. Schimmel. 1980. Biophysical Chemistry. Part II: Techniques for the study of Biological Structure and Function. W. H. Freeman, New York. 560–567.

Cole, N. B., C. L. Smith, N. Sciaky, M. Terasaki, M. Edidin, and J. Lippincott-Schwartz. 1996. Diffusional mobility of Golgi proteins in membranes of living cells. *Science*. 273:797–801.

Cox, J. S., R. E. Chapman, and P. Walter. 1997. The unfolded protein response coordinates the production of endoplasmic reticulum protein and endoplasmic reticulum membrane. *Mol. Biol. Cell*. 8:1805–1814.

Crank, J. 1975. The Mathematics of Diffusion, 2nd Ed. Oxford University Press, New York. 29.

DeGiorgi, F., M. Brini, C. Bastianutto, R. Marsault, M. Montero, P. Pizzo, R. Rozzi, and R. Rizzuto. 1996. Targeting aequorin and green fluorescent protein to intracellular organelles. *Gene*. 173:113–117.

Ellenberg, J., E. D. Siggia, J. E. Moreira, C. L. Smith, J. F. Presley, H. J. Worman, and J. Lippincott-Schwartz. 1997. Nuclear membrane dynamics and reassembly in living cells: targeting of an inner nuclear membrane protein in interphase and mitosis. *J. Cell. Biol.* 138:1193–1206.

Farinas, J., V. Simenak, and A. S. Verkman. 1995. Cell volume measured in adherent cells by total internal reflection microfluorimetry: application to permeability in cells transfected with water channel homologs. *Biophys. J.* 68:1613–1620.

Feder, T. J., I. Brust-Mascher, J. P. Slattery, B. Baird, and W. W. Webb. 1996. Constrained diffusion or immobile fraction on cell surfaces: a new interpretation. *Biophys. J.* 70:2367–2373.

Fushimi, K., and A. S. Verkman. 1991. Low viscosity in the aqueous domain of cytoplasm measured by picosecond polarization microscopy. *J. Cell Biol.* 112:719–725.

Gerdes, H.-H., and C. Kaether. 1996. Green fluorescent protein: applications to cell biology. *FEBS Lett.* 389:44–47.

Griffiths, G., M. Ericsson, J. Krijnse-Locker, T. Nilsson, B. Goud, H. D. Sàling, B. L. Tang, S. H. Wong, and W. Hong. 1994. Localization of the Lys, Asp, Glu, Leu tetrapeptide receptor to the Golgi complex and the intermediate compartment in mammalian cells. *J. Cell Biol.* 127: 1557–1574.

Hammond, C., and A. Helenius. 1995. Quality control in the secretory pathway. *Curr. Opin. Cell Biol.* 7:525–539.

Helenius, A., T. Marquardt, and I. Braakman. 1992. The endoplasmic reticulum as a protein-folding compartment. *Trends Cell Biol.* 2:227–231.

Kao, H. P., J. R. Abney, and A. S. Verkman. 1993. Determinants of the translational diffusion of a small solute in cytoplasm. *J. Cell Biol.* 120:175–184.

Kao, H. P., and A. S. Verkman. 1996. Construction and performance of a FRAP instrument with microsecond time resolution. *Biophys. Chem.* 59:203–210.

Klausner, R. D., J. G. Donaldson, and J. Lippincott-Schwartz. 1992. Brefeldin A: insights into the control of membrane traffic and organelle structure. *J. Cell Biol.* 116:1071–1080.

Kneen, M., J. Farinas, Y. Li, and A. S. Verkman. 1998. Green fluorescent protein as a noninvasive intracellular pH indicator. *Biophys. J.* 74: 1591–1600.

Koch, G. L. E., D. R. J. Macer, and M. J. Smith. 1987. Visualization of the intact endoplasmic reticulum by immunofluorescence with antibodies to the major ER glycoprotein, endoplasmin. *J. Cell. Sci.* 87:535–542.

Lee, C., and L. B. Chen. 1988. Dynamic behavior of endoplasmic reticulum in living cells. *Cell* 54:37–46.

Luby-Phelps, K., P. E. Castle, D. L. Taylor, and F. Lanni. 1987. Hindered diffusion of inert tracer particles in the cytoplasm of mouse 3T3 fibroblasts. *Proc. Natl. Acad. Sci. USA.* 84:4910–4913.

Luby-Phelps, K., S. Mujundar, R. Mujundar, L. Ernst, W. Galbraith, and A. Waggoner. 1993. A novel fluorescence ratiometric method confirms the low solvent viscosity of the cytoplasm. *Biophys. J.* 65:236–242.

McMillan, D. R., M. J. Gething, and J. Sambrook. 1994. The cellular response to unfolded proteins: intercompartmental signaling. *Curr. Opin. Biotechnol.* 5:540–545.

Ölveczky, B. P., and A. S. Verkman. 1998. Monte Carlo analysis of obstructed diffusion in three dimensions: application to molecular diffusion in organelles. *Biophys. J.* 74:2722–2730.

Ormø, M., A. B. Cubitt, K. Kallio, L. A. Gross, R. Y. Tsien, and S. J. Remington. 1996. Crystal structure of the *Aequorea victoria* green fluorescent protein. *Science*. 273:1392–1395.

Partikian, A., B. Ölveczky, R. Swaminathan, Y. Li, and A. S. Verkman. 1998. Rapid diffusion of green fluorescent protein in the mitochondrial matrix. *J. Cell Biol.* 140:821–829.

Periasamy, N., S. Bicknese, and A. S. Verkman. 1996. Reversible photobleaching of fluorescein conjugates in air-saturated viscous solutions: molecular tryptophan as a triplet state quencher. *Photochem. Photobiol.* 63:265–271.

Periasamy, N., and A. S. Verkman. 1998. Analysis of fluorophore diffusion by continuous distributions of diffusion coefficients: application to photobleaching measurements of simple and anomalous diffusion. *Biophys. J.* 75:557–567.

Presley, J. F., N. B. Cole., T. A. Schroer, K. Hirschberg, K. J. M. Zaal, and J. Lippincott-Schwartz. 1997. ER to Golgi transport visualized in living cells: microtubule dependent translocation of tubulovesiclar intermediates. *Nature.* 389:81–85.

Rizzuto, R., M. Brini, P. Pizzo, M. Murgia, and T. Pozzan. 1995. Chimeric green fluorescent protein as a tool for visualizing subcellular organelles in living cells. *Curr. Biol.* 5:636–642.

Sciaky, N., J. Presley, C. Smith, K. J. M. Zaal, N. Cole, J. E. Moreira, M. Terasaki, E. Siggia, and J. Lippincott-Schwartz. 1997. Golgi tubule traffic and the effects of brefeldin A visualized in living cells. *J. Cell Biol.* 139:1137–1155.

Seksek, O., J. Biwersi, and A. S. Verkman. 1997. Translational diffusion of macromolecule-size solutes in cytoplasm and nucleus. *J. Cell. Biol.* 138:131–142.

Simon, S., C. S. Peskin, and G. F. Oster. 1992. What drives the translocation of proteins? *Proc. Natl. Acad. Sci. U.S.A.* 89:3770–3774.

Stinchcombe, J. C., H. Nomoto, D. F. Cutler, and C. R. Hopkins. 1995. Anterograde and retrograde traffic between the rough endoplasmic reticulum and the Golgi complex. *J. Cell Biol.* 131:1387–1401.

Subramanian, K., and T. Meyer. 1997. Calcium-induced restructuring of nuclear envelope and endoplasmic reticulum calcium stores. *Cell.* 89: 963–71.

Swaminathan, R., S. Bicknese, N. Periasamy, and A. S. Verkman. 1996. Cytoplasmic viscosity near the cell plasma membrane: translation of BCECF measured by total internal reflection-fluorescence photobleaching recovery. *Biophys. J.* 71:1140–1151.

Swaminathan, R., C. P. Hoang, and A. S. Verkman. 1997. Photochemical properties of green fluorescent protein GFP-S65T in solution and transfected CHO cells: analysis of cytoplasmic viscosity by GFP translational and rotational diffusion. *Biophys. J.* 72:1900–1907.

Tamarappoo, B. K., and A. S. Verkman. 1998. Defective trafficking of AQP2 water channels in nephrogenic diabetes insipidus and correction by chemical chaperones. *J. Clin. Invest.* 101:2257–2267.

Terasaki, M., L. A. Jaffe, G. R. Hunnicutt, and J. A. Hammer. 1996. Structural change of the endoplasmic reticulum during fertilization: evidence for loss of membrane continuity using the green fluorescent protein. *Dev. Biol.* 179:320–328.

Verkman, A. S. 1999. Green fluorescent protein as a probe to study intracellular solute diffusion. *Meth. Enzymol* 302:250–265.

Verkman, A. S., M. Armijo, and K. Fushimi. 1991. Construction and evaluation of a frequency-domain epifluorescence microscope for lifetime and anisotropy decay measurements in subcellular domains. *Biophys. Chem.* 40:117–125.

Weast, R. C., editor. 1986. CRC Handbook of Chemistry and Physics, 67th Ed. CRC Press, Boca Raton.

Yang, F., L. G. Moss, and G. N. Phillips. 1996. The molecular structure of green fluorescent protein. *Nature Biotech.* 14:1264–1251.